Universality and scaling study of the critical behavior of the two-dimensional Blume-Capel model in short-time dynamics

Roberto da Silva,* Nelson A. Alves,[†] and J. R. Drugowich de Felício[‡]

Departamento de Física e Matemática, FFCLRP Universidade de São Paulo, Avenida Bandeirantes 3900,
CEP 014040-901 Ribeirão Preto, São Paulo, Brazil

In this paper we study the short-time behavior of the Blume-Capel model at the tricritical point as well as along the second order critical line. Dynamic and static exponents are estimated by exploring scaling relations for the magnetization and its moments at an early stage of the dynamic evolution. Our estimates for the dynamic exponents, at the tricritical point, are $z = 2.215(2)$ and $\theta = -0.53(2)$.

I. INTRODUCTION

Numerical simulation in the short-time regime has become an important tool to study phase transitions and critical phenomena. The reason is that universality and scaling behavior are already present in the dynamic systems since the early stages of their evolution [1,2]. Moreover, this kind of approach reveals the existence of a new and unsuspected critical exponent. As shown by Janssen *et al.* [1] on the basis of renormalization group theory, if the parameters are adjusted to their critical values but with initial configurations characterized by nonequilibrium states, the time evolution of quantities such as magnetization exhibits a polynomial behavior governed by an exponent θ, which is independent of the known set of static exponents and of the dynamical critical exponent z. This new exponent characterizes the so called "critical initial slip," the anomalous behavior of the magnetization when the system is quenched to the critical temperature T_c. Working with systems without conserved quantities, model A in the terminology of Halperin *et al.* [3], Janssen *et al.* found a scaling form for the moments of the magnetization, which sets soon after a microscopic time scale t_{mic}. Those relations have been confirmed in several numerical experiments [4–6]. For the kth moment of the magnetization, this scaling form reads

$$M^{(k)}(t,\tau,L,m_0) = b^{-k\beta/\nu}M^{(k)}(b^{-z}t,b^{1/\nu}\tau,b^{-1}L,b^{x_0}m_0). \tag{1}$$

Here b is an arbitrary spatial scaling factor, t is the time evolution, and τ is the reduced temperature, $\tau = (T - T_c)/T_c$. As usual, the exponents β and ν are the well-known static exponents, and z is the dynamic one. Equation (1) depends on the initial magnetization m_0 and gives origin to the new exponent x_0, the scaling dimension of the initial magnetization, related to θ by $x_0 = z\theta + \beta/\nu$.

For a large lattice size L and small initial magnetization m_0, the system in its early stage presents small spatial and temporal correlation lengths, which may eliminate usual finite size problems. In this limit, if we choose the scaling factor $b = t^{1/z}$ [1,5,6] at the critical temperature ($\tau = 0$), we obtain

$$M(t,m_0) \sim m_0 t^\theta \tag{2}$$

from the scaling relation (1). The exponent θ has been calculated for the two-dimensional (2D) [5,7] and three-dimensional (3D) [7,8] Ising models, 2D three-state Potts model [5], Ising model with next-nearest-neighbor interactions [9], and Ising model with a line of defects [10]. In addition, this short-time universal behavior was found in irreversible models with synchronous [11] and continuous time dynamics [12]. In all of those cases, a positive value for θ has been found, indicating a surprising initial increase of the magnetization in the short-time regime $t_{mic} < t < t_i \sim m_0^{-z/x_0}$. This effect can be related to a "mean field" (MF) behavior since the system presents small correlation length in the beginning of the time evolution. Thus, when the system is quenched to the critical temperature T_c, it behaves as in an ordered state since $T_c < T_c^{(MF)}$ [13].

On the other hand, as shown by Janssen and Oerding [14], the behavior of a thermodynamic system is more complex at a tricritical point, where the corresponding exponent θ may attain negative values.

At a tricritical point the magnetization shows a crossover from the logarithmic behavior $M(t) \sim m_0[\ln(t/t_0)]^{-a}$, (where a is an universal exponent) at short times $t_0 \equiv t_{mic} \ll t \ll m_0^{-4}$ to long-time $t^{-1/4}$ power law behavior with logarithmic corrections, $M(t) \sim [t/\ln(t/t_0)]^{-1/4}$ in three dimensions. This behavior can be stated in the generalized form

$$M(t) = m_0[\ln(t/t_0)]^{-a}F_M\!\left(\!\left(\frac{t}{\ln(t/t_0)}\right)^{1/4}[\ln(t/t_0)]^{-a}m_0\right), \tag{3}$$

where $F_M(x) \sim 1$ or $F_M(x) \sim 1/x$, respectively, for vanishing and large arguments. Below three dimensions it reduces to the scaling form

$$M(t) \sim m_0 t^\theta. \tag{4}$$

_____

*Email address: rsilva@dfm.ffclrp.usp.br

[†]Email address: alves@quark.ffclrp.usp.br

[‡]Email address: drugo@usp.br

Here θ is the exponent related to the tricritical point of the relaxation process at early times which is expected to assume negative values.

In this paper, we perform short-time Monte Carlo (MC) simulations to explore the critical dynamics of the 2D Blume-Capel model. We evaluate the dynamic exponents θ and z, as well as the static exponents ν and β at the tricritical point. To the best of our knowledge, this is the first time it is done numerically. We also estimate the dynamic exponents along the second order critical line. We observe a clear trend toward the values of z and θ for the corresponding 2D Ising values when the crystal field D becomes large and negative, indicating dynamic universality along the critical line in the limit $D \rightarrow -\infty$.

In the following section we present the model and its phase diagram. Section III contains the main scaling relations and describes our short-time MC simulations. Results are presented for critical points on the second-order transition line. In Sec. IV, we explore the short-time dynamics at the tricritical point. Section V contains a brief outlook and concluding remarks.

II. THE MODEL

The Blume-Capel [15] (BC) model is a spin-1 model which has been used to describe the behavior of ^{3}He-^{4}He mixtures along the λ line and near the critical mixing point. Apart from its practical interest, the BC model has intrinsic interest since it is the simplest generalization of the Ising model ($s=1/2$) exhibiting a rich phase diagram with first and second-order transition lines as well as a tricritical point. Tricritical points appear in ^{3}He-^{4}He mixtures such that when a small fraction of ^{3}He is added to ^{4}He, a critical line terminates at a concentration of ^{3}He approximately at 0.67. The BC model, or its well known generalization, the Blume-Emery-Griffiths model [16,17], was studied by mean-field approximation, real space renormalization group schemes [18], Monte Carlo renormalization group approach [19], and finite-size scaling combined with conformal invariance [20–22]. The Hamiltonian of the two-dimensional model is

$$H = -J \sum_{\langle i,j \rangle} S_i S_j + D \sum_{i=1} S_i^2, \tag{5}$$

where $\langle i,j \rangle$ indicates nearest neighbors on L^2 lattices and $S_i = \{-1, 0, 1\}$. The parameter J is the exchange coupling constant and D is the crystal field. We show its phase diagram in Fig. 1. Table I lists points D/J on the second order critical line and at the tricritical point where we have performed our simulations. Those points in Table I were obtained from [23] and from a private communication [22]. Table I also contains our results for the corresponding critical and tricritical exponents.

We remark that along the critical line, this model presents a critical behavior similar to that of the Ising model. However, exactly at the tricritical point the exponents change abruptly. They are given by the dimensions of the irreducible representations of Virasoro algebra [24,25] with central charge (conformal anomaly number) $c=7/10$ [21]. Finite-
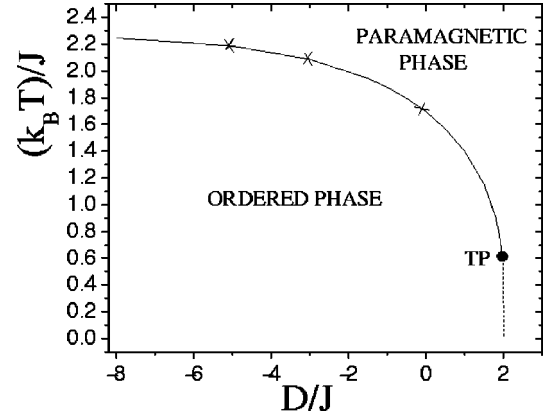
FIG. 1. Phase diagram of the Blume-Capel model. The dashed curve is a first-order transition line and the solid curve is a second order one. These curves are connected by a tricritical point (TP). The marked points ($\times$, $\bullet$) correspond to the simulated values.

size scaling combined with conformal invariance [20] permitted to observe a smooth transition between Ising-like and tricritical behavior. In finite systems, Ising-like behavior is reached only when $D \rightarrow -\infty$. In that limit $\beta/(2-1/\nu) \rightarrow 0.125$, the exact value for the Ising model. In our short-time simulations the same kind of Ising-like behavior is observed for the dynamic exponents z and θ as we move along the critical line.

III. NONEQUILIBRIUM SHORT-TIME DYNAMICS AT A CRITICAL POINT

In short-time MC simulations critical slowing down can be neglected because spatial and time correlation lengths are small in the early stages of evolution. On the other hand, we need to deal with several samples with independent initial configurations since the systems are far from equilibrium. In fact, this approach requires calculation of the average (over samples) of the magnetization and of its moments $M^{(k)}(t)$,

$$M^{(k)}(t) = \frac{1}{N_S L^{kd}} \sum_{j=1}^{N_S} \left(\sum_{i=1}^{L^d} S_{ij}(t) \right)^k, \tag{6}$$

where $S_{ij}(t)$ denotes the spin i of the jth sample at the tth MC sweep. Here N_S denotes the number of samples and L^d is the volume of the system. This kind of simulation is performed N_B times to obtain our final estimates as a function of t. In this paper, the dynamic evolution of the spins $\{S_i\}$ is local and updated by the heat-bath algorithm.

A. The critical initial slip

The evolution of the kth moment of magnetization in the initial stage of the dynamic relaxation can be obtained from Eq. (1) for large lattice sizes L at $\tau=0$ with $b=t^{1/z}$. This yields

$$M^{(k)}(t, m_0) = t^{-k\beta/\nu z} M^{(k)}(1, t^{x_0/z} m_0). \tag{7}$$

TABLE I. Critical parameters and exponents for the 2D Blume-Capel model.

D/J	$k_B T/J$	θ [Eq. (8)]	z [Eq. (12)]	z [Eq. (16)]	$1/\nu$ [Eqs. (17) and (12)]	$1/\nu$ [Eqs. (17) and (16)]	β [Eq. (14)]
Critical points							
0	1.6950	0.194(3)	2.16(2)	2.106(2)	0.99(2)	0.97(2)	0.134(2)
-3	2.0855	0.193(5)	2.16(1)	2.128(2)	1.00(1)	0.99(1)	0.125(2)
-5	2.1855	0.187(5)	2.15(1)	2.139(2)	1.00(3)	0.99(3)	0.125(4)
Tricritical point							
1.9655	0.610	$-0.53(2)$	2.21(2)	2.215(2)	1.86(2)	1.864(6)	0.0453(2)

By expanding the corresponding first moment equation for small m_0, we obtain Eq. (2) under the condition that $t^{x_0/z} m_0$ is sufficiently small, which sets a time scale $t_i \sim m_0^{-z/x_0}$ [1,4,6] where that phenomena can be observed.

In Fig. 2(a) we present our results for the exponent θ at the critical point $k_B T_c/J = 1.6950$ and $D_c/J = 0$, for lattice size $L = 80$ and five different initial magnetizations m_0. Our estimates for each $\theta = \theta(m_0)$ were obtained from $N_B = 5$ independent bins with $N_S = 10\,000$, for t up to 100 sweeps. Figure 2(b) illustrates the determination of θ for $m_0 = 0.02$ from a log-log plot of the magnetization versus time. The linear fitting in Fig. 2(a) gives $\theta = 0.193(2)$ (not presented in Table I) with goodness of fit [26] $Q = 0.72$.
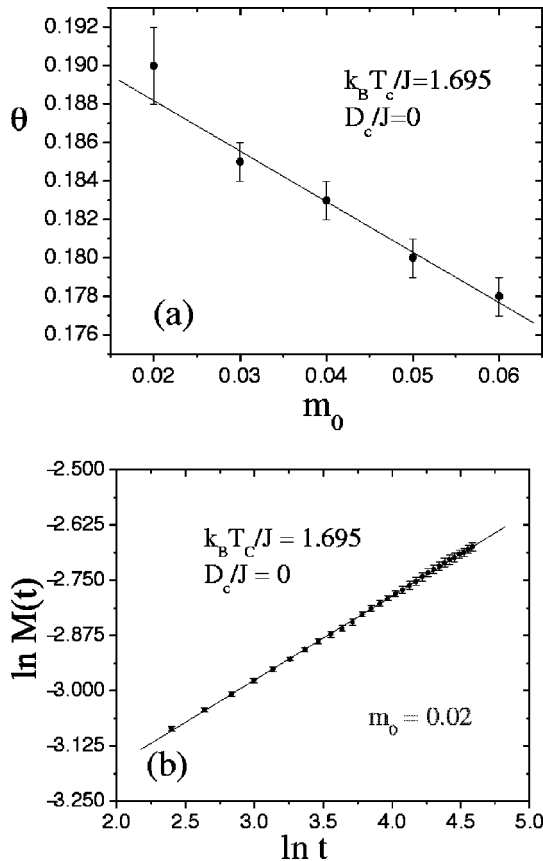
FIG. 2. (a) Exponent θ in function of initial magnetization m_0 for square lattices with $L = 80$. The straight line is a least-square fit to the data. (b) Time evolution of the magnetization for $L = 80$ and $m_0 = 0.02$.

Another method has been recently proposed by Tomé and de Oliveira [27] to evaluate θ. It avoids the sharp preparation of samples with defined and nonzero magnetization and the delicate numerical extrapolation $m_0 \to 0$. The method is based on the time correlation function of the total magnetization,

$$C(t) = \frac{1}{L^d} \left\langle \sum_{i=1}^{L^d} \sum_{j=1}^{L^d} S_i(t) S_j(0) \right\rangle. \qquad (8)$$

Starting from random initial configurations the above correlation behaves as $C(t) \sim t^\theta$, which permits us to obtain the exponent θ from a log-log plot of $C(t)$ versus t. We obtained $\theta = 0.194(3)$ for $k_B T_c/J = 1.6950$ and $D_c/J = 0$ choosing the time interval $[20\text{--}150]$ in which the value of Q ($Q = 0.99$) was highest. This value is in complete agreement with our above estimate of the exponent θ and it is consistent within error bars with previous results for the 2D Ising model. In Table I we also present results for θ at other points of the critical line.

B. Dynamic critical exponent z

The observables in short-time analysis are described by different scaling relations according to the initial magnetizations. In particular, the second moment $M^{(2)}(t,L)$ in Eq. (6),

$$M^{(2)} = \frac{1}{L^{2d}} \left\langle \sum_{i=1}^{L^d} S_i^2 \right\rangle + \frac{1}{L^{2d}} \sum_{i \neq j}^{L^d} \langle S_i S_j \rangle, \qquad (9)$$

with $m_0 = 0$ behaves as L^{-d} since in the short-time evolution the spatial correlation length is very small when compared with the lattice size L. Thus, one arrives at [5,6]

$$M^{(2)}(t,L) = t^{-2\beta/\nu z} M^{(2)}(1, t^{-1/z} L) \sim t^{(d - 2\beta/\nu)/z}. \qquad (10)$$

This equation can be used to determine relations involving the static critical exponents and the dynamic exponent z [6,28]. However, a way to evaluate independently the exponent z is through the time-dependent fourth-order Binder cumulant at the critical temperature ($\tau = 0$),

$$U_4(t,L,m_0) = 1 - \frac{M^{(4)}(t,L,m_0)}{3[M^{(2)}(t,L,m_0)]^2}, \qquad (11)$$

which obeys the equation
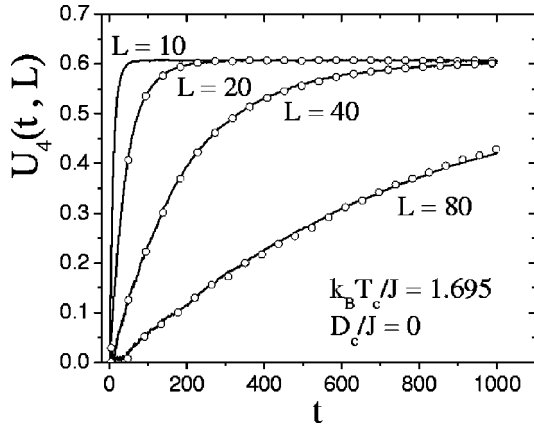
FIG. 3. Cumulants $U_4(t,L)$ for $L=10$, 20, 40, and 80 for initial magnetization $m_0=0$. The open circles on the lines show the cumulants for lattice sizes $L/2$ rescaled in time with z obtained from Eq. (13).

$$U_4(t,L,m_0)=U_4(b^{-z}t,b^{-1}L,b^{x_0}m_0). \qquad (12)$$

If we set $m_0=0$, we eliminate the dependence on the exponent x_0 and the exponent z can be evaluated through scaling collapses of the generalized cumulant for different lattice sizes [4,29]. To match the Binder cumulants $U_4(t_1,L_1)$ and $U_4(t_2,L_2)$ obtained from two time series for lattice sizes L_1 and L_2, with $b=L_2/L_1$ $(L_2>L_1)$, we interpolate the series $U_4(t,L_1)$ to obtain $\tilde{U}_4(b^{-z}t,L_1)$. Next, we define the function

$$\chi^2(z)=\frac{1}{t_f-t_i}\sum_{t=t_i}^{t_f}[\tilde{U}_4(b^{-z}t,L_1)-U_4(t,L_2)]^2, \qquad (13)$$

where the best estimate for z corresponds to the one which minimizes $\chi^2(z)$.

In Fig. 3 we show the scaling collapses of the Binder cumulants for the following pairs of lattices (L_1,L_2) $=(10,20),(20,40)$, and $(40,80)$ at $k_BT_c/J=1.6950$, and $D_c/J=0$. From the largest pair of lattices we obtained $z=2.16(2)$ in the time interval $[50-1000]$. Our error estimate is based on different collapses obtained from $N_B=5$ independent bins for each lattice size.

Another universal behavior of the dynamic relaxation process also described by Eq. (1) can be obtained with the initial condition $m_0=1$ [30–32]. This condition is related to another fixed point in the context of renormalization group approach. Thus, starting from an initial ordered state one obtains a power law decay of the magnetization at the critical temperature,

$$M(t)\sim t^{-\beta/\nu z}, \qquad (14)$$

when we choose $b^{-z}t=1$ in the limit of $L\rightarrow\infty$. Taking into account this relation, another method has been proposed [6] to estimate the dynamic exponent z. This approach uses the second order cumulant
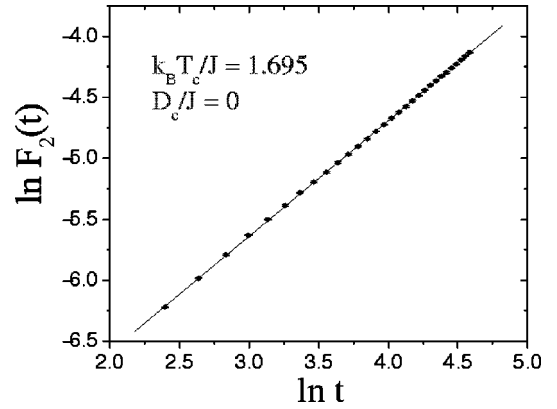
FIG. 4. Time evolution of $F_2(t)$ for $L=160$ with mixed initial conditions [Eq. (16)].

$$U_2(t,L)=\frac{M^{(2)}(t,L)}{[M(t,L)]^2}-1, \qquad (15)$$

which should take the simple form $U_2(t,L\rightarrow\infty)\sim t^{d/z}$. The advantage of this procedure is that curves for different lattices lie on the same straight line in a log-log plot without any rescaling in time. However, this technique has not been successful in at least two well known models: the two-dimensional $q=3$ Potts model [6] and the Ising model with three spin interactions in just one direction [10]. The reason for the above disagreement may be related to the behavior of Eq. (9) when $m_0=1$. We have proposed [33] that this scaling form $t^{d/z}$ could indeed be obtained working with the ratio $F_2=M^{(2)}/M^2$ with different initial conditions for each moment since we know the behavior of the second moment of the magnetization when samples are initially disordered $(m_0=0)$ and also the time dependence of the magnetization when samples are initially ordered $(m_0=1)$. Therefore, we obtain a mixed function

$$F_2(t)=\frac{M^{(2)}(t,L)|_{m_0=0}}{[M(t,L)]^2|_{m_0=1}}\sim t^{d/z}. \qquad (16)$$

A log-log plot with error bars for the critical point $k_BT_c/J=1.6950$ and $D_c/J=0$ is presented in Fig. 4 for $L=160$. We obtained $z=2.106(2)$ with $Q=0.99$ in the range $[30-200]$, which does not agree with the value obtained from Eq. (12). However, as we move away from the tricritical point, the values of z obtained (Table I) with Eq. (16) show a clear trend toward the expected value of the dynamic exponent z [$z=2.156(2)$] of the 2D Ising model [33]. On the other hand, the values obtained from the cumulant in Eq. (12) remain essentially the same along the entire critical line.

C. Static exponents and universality class

The exponent $1/\nu z$ can be obtained by differentiating $\ln M(t,\tau,m_0)$ with respect to the temperature at T_c,

$$\frac{\partial \ln M(t,\tau,L)}{\partial\tau}\bigg|_{\tau=0}\sim t^{1/\nu z}, \qquad (17)$$
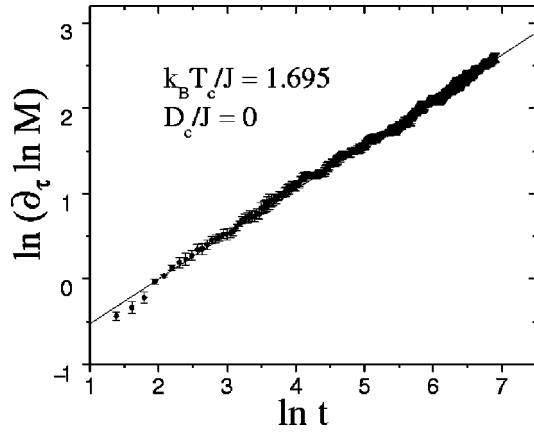
FIG. 5. Time evolution of the derivative $\partial_\tau \ln M(t,\tau)|_{\tau=0}$ for $L=160$ and initial magnetization $m_0=1$.

if we consider the scaling relation for the magnetization when the initial state of samples is ordered ($m_0=1$) [29].

Our results for νz were obtained through finite differences at $T_c \pm \delta$ with $\delta=0.001$. They rely on $N_B=5$ independent bins with $N_S=5000$ samples each for $L=160$. The time interval [80–200] corresponds to the range where the goodness of fit parameter attains its highest value ($Q=0.99$).

In Fig. 5 we show the log-log behavior of the derivative $\partial_\tau \ln M(t)$ at $k_B T_c/J=1.6950$ and $D_c/J=0$. In Table I we present our final estimates of $1/\nu$. The sixth column is obtained with the estimates of z from Eq. (12) (data in fourth column), while the seventh column corresponds to estimates for ν with values of z from Eq. (16) (data in fifth column).

Since we have already collected estimates for νz [Eq. (17)], it is straightforward to obtain estimates for β following Eq. (14). Our estimates of β are presented in the last column. Our values in Table I can be compared with theoretical predictions for an Ising-like critical point ($1/\nu=1, \beta=1/8$).

IV. RESULTS FROM SHORT-TIME DYNAMICS AT THE TRICRITICAL POINT

From the results presented in Refs. [1] and [14] we can describe the time dependence of the first moment of the magnetization for the 2D Blume-Capel model as

$$M(t) \sim \begin{cases} m_0 t^\theta, & t_{mic} < t < t_i, \\ t^{-\beta/\nu z}, & t_i < t < t_\tau, \end{cases} \qquad (18)$$

for an initial small magnetization m_0, where $\theta>0$ ($\theta<0$) identifies a critical (tricritical) point. Here t_τ stands for the time before the system has reached thermal equilibrium.

We also included in Table I our estimates for $\theta, z, 1/\nu$ and β at the tricritical point $k_B T_t/J=0.610$, and $D_t/J=1.9655$, for lattice size $L=80$.

In Fig. 6 we show the values of θ for five different initial magnetizations m_0 at the tricritical point. Our estimates for each $\theta(m_0)$ were obtained from $N_B=20$ independent bins with $N_S=10\,000$ samples, for t up to 80 sweeps. The least-square fit to data in Fig. 6 gives $\theta=-0.53(2)$ with goodness
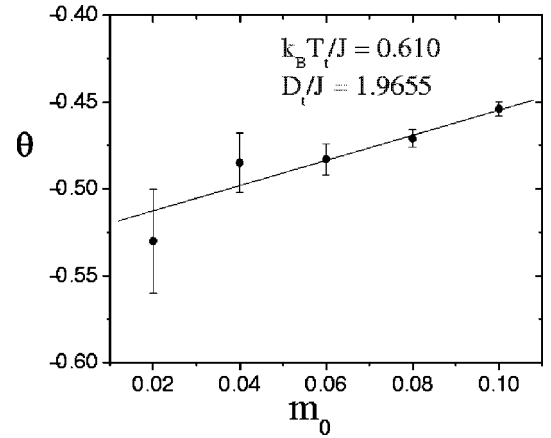
FIG. 6. Exponent θ in function of initial magnetizations m_0 for $L=80$ at the tricritical point. The straight line is a least-square fit to the data.

of fit $Q=0.75$. The corresponding study with the time correlation function $C(t)$ in Eq. (8) also gives $\theta=-0.53(2)$ with $Q=0.99$ in the time interval [20–80]. Data are shown in Fig. 7.

We have checked further this value for θ calculating the spin-spin autocorrelation function

$$A(t) = \frac{1}{L^d} \left\langle \sum_i S_i(0) S_i(t) \right\rangle \sim t^{-(d/z-\theta)}. \qquad (19)$$

Our data analysis as a function of t (see Fig. 8) gives $d/z -\theta=1.457(6)$, with acceptable Q ($Q=0.56$), coincidently in the same time interval [20–80], with $N_S=20\,000$ samples. If we take in advance our estimates for z presented below, this result leads to $\theta=-0.55(2)$ or to $\theta=-0.554(6)$, respectively, for $z=2.21(2)$ and $z=2.215(2)$, corroborating our independent estimate of θ at the tricritical point.

The generalization of the dynamic scaling relation for the kth moment of the magnetization at a tricritical point can be written as [34]
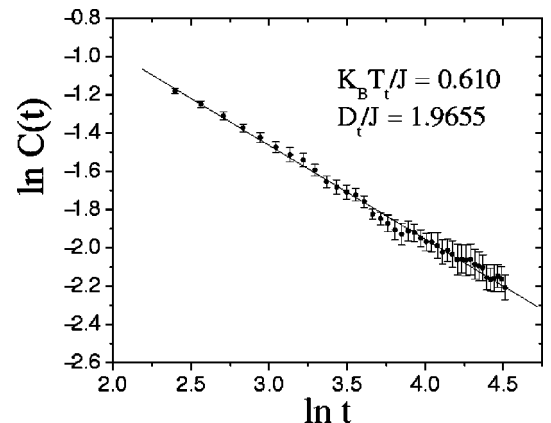
FIG. 7. Time correlation function $C(t)$ at the tricritical point.
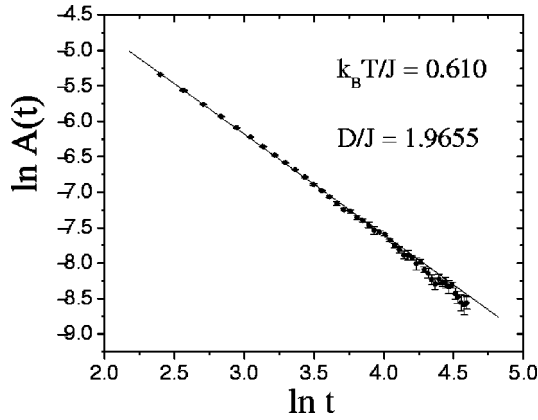
FIG. 8. Autocorrelation function $A(t)$ at the tricritical point.

$$M^{(k)}(t,\tau,g,L,m_0)$$
$$= b^{-k\beta_t/\nu}M^{(k)}(b^{-z}t,b^{1/\nu}\tau,b^{\phi_t/\nu}g,b^{-1}L,b^{x_0}m_0).$$
$$(20)$$

It differs from the critical case by the scaling field g that measures the deviation from the transition line at the tricritical point. The quantity ϕ_t is known as the crossover exponent. At tricriticality $t=g=0$.

We show in Fig. 9 scaling collapses of the cumulant $U_4(t,L)$ at the tricritical point, quite different than the scaling collapses at a critical point (Fig. 3). Our estimate based on Eq. (12) leads to $z=2.21(2)$ obtained from the pair of largest lattice sizes $L=40$ and 80. The value is the same for time intervals $[10,1000]$ and $[200,1000]$. Another estimate for the dynamic exponent, based on Eq. (16) gives $z=2.215(2)$ obtained from a larger lattice ($L=160$) in the time interval $[30,200]$, with $Q=0.71$. We do not show the log-log plot of $F_2(t)$ in this case because it is quite similar to Fig. 4. We had to restrict the time interval, when compared with the U_4 calculation, in order to obtain acceptable values for Q. Here, in contrast to the different estimates of z (fourth and fifth column) at the critical points listed in Table I, both methods lead to the same estimate for z.
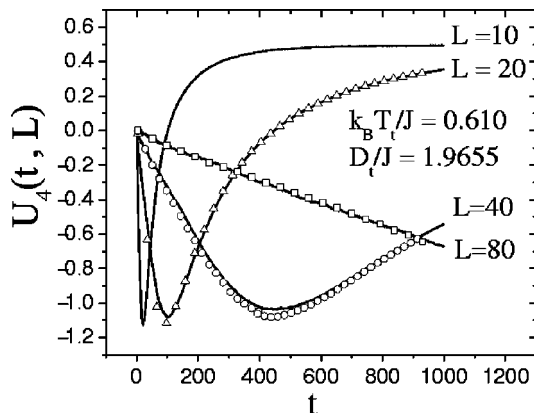
FIG. 9. Cumulants $U_4(t,L)$ for $L=10$, 20, 40, and 80 for an initial magnetization $m_0=0$ at the tricritical point. The symbols on the lines show the cumulants with lattice sizes $L/2$ rescaled in time with z given by Eq. (13).

The evaluation of static exponents ν and β at the tricritical point follows the same procedure as applied on the critical line. Estimates exhibited in Table I are in good agreement with results provided by conformal invariance [21,24] $1/\nu=9/5$ and $\beta=1/24$.

Next, in order to study the influence of the local dynamics on the values of the exponents we recall the simulations with Glauber dynamics performed by Bonfim [34]. Our estimate of $\beta/\nu z$ obtained from the decay of the magnetization (starting from initially ordered state) is 0.0381(1) with the heat-bath dynamics, whereas the value quoted by Bonfim who used Glauber update is 0.037 67(73), reinforcing the dynamic universality also for tricritical behavior.

V. CONCLUSIONS

We have performed short-time Monte Carlo simulations to evaluate dynamic and static exponents at critical and tricritical points of the spin-1 Blume-Capel model.

According to analytical predictions by Janssen and Oerding, a negative value for the new exponent θ was obtained at the tricritical point. In order to confirm that prediction we calculated θ by three different techniques: (i) directly, by following the power law behavior $M(t)\propto m_0 t^\theta$ when the samples are sharply prepared with a small initial magnetization m_0; (ii) studying the time correlation of the magnetization $C(t)$ which also evolves in time like t^θ, and (iii) calculating the autocorrelation function $A(t)$ which decays like $t^{-(d/z-\theta)}$ where $d=2$ in the present case and z is the dynamical critical exponent at the tricritical point. All of our estimates for θ, at the tricritical point, are in the range $-0.57 \leq \theta \leq -0.51$. The dynamic exponent z was also calculated by different techniques: first by collapsing the fourth-order Binder cumulant U_4 for several pairs of lattices, and second by following the ratio $F_2(t)$ which explores scaling laws for the moments of the magnetization under mixed initial conditions. Both methods lead essentially to the same value (2.21) but the error bar in the second case is ten times smaller than that obtained by the Binder cumulant. The value of z was used to obtain the static exponents β and ν, in good agreement with exact values provided by conformal invariance.

Dynamic exponents were also calculated along the second-order critical line. Estimates for θ and z are in good agreement with the results for the 2D Ising model, indicating that universality stays valid in the dynamic level. However, it is worthwhile to mention that the recently proposed technique [33] based on mixed initial conditions is more sensitive to crossover effects than fourth-order Binder cumulant.

ACKNOWLEDGMENTS

[1] H.K. Janssen, B. Schaub, and B. Schmittmann, Z. Phys. B: Condens. Matter **73**, 539 (1989).

[2] D.A. Huse, Phys. Rev. B **40**, 304 (1989).

[3] B.I. Halperin, P.C. Hohenberg, and S-K. Ma, Phys. Rev. B **10**, 139 (1974).

[4] Z.B. Li, L. Schülke, and B. Zheng, Phys. Rev. Lett. **74**, 3396 (1995).

[5] K. Okano, L. Schülke, K. Yamagishi, and B. Zheng, Nucl. Phys. B: Field Theory Stat. Syst. **485[FS]**, 727 (1997).

[6] B. Zheng, Int. J. Mod. Phys. B **12**, 1419 (1998).

[7] P. Grassberger, Physica A **214**, 547 (1995); A. Jaster, J. Mainville, L. Schülke, and B. Zheng, J. Phys. A **32**, 1395 (1999).

[8] Z.B. Li, U. Ritschel, and B. Zheng, J. Phys. A **27**, L837 (1994).

[9] A.J. Ye, Z.G. Pan, Y. Chen, and Z.B. Li, Commun. Theor. Phys. **33**, 205 (2000).

[10] C.S. Simões and J.R. Drugowich de Felício, J. Phys. A **31**, 7265 (1998); T. Tomé, C.S. Simões, and J.R. Drugowich de Felício, Mod. Phys. Lett. B **15**, 487 (2001).

[11] T. Tomé and J.R. Drugowich de Felício, Mod. Phys. Lett. B **12**, 873 (1998).

[12] J.F.F. Mendes and M.A. Santos, Phys. Rev. E **57**, 108 (1998).

[13] J.B. Zhang, L. Wang, D.W. Gu, H.P. Ying, and D.R. Ji, Phys. Lett. A **262**, 226 (1999), and references therein.

[14] H.K. Janssen and K. Oerding, J. Phys. A **27**, 715 (1994).

[15] M. Blume, Phys. Rev. **141**, 517 (1966); H.W. Capel, Physica (Amsterdam) **32**, 966 (1966); **33**, 295 (1967); **37**, 423 (1967).

[16] M. Blume, V.J. Emery, and R.B. Griffiths, Phys. Rev. A **4**, 1071 (1971).

[17] I. D. Lawrie and S. Sarbach, in *Phase Transitions and Critical Phenomena*, edited by C. Domb and J. L. Lebowitz (Academic, London, 1984), Vol. 9.

[18] A.N. Berker and M. Wortis, Phys. Rev. B **14**, 4969 (1976); T.W. Burkhardt, *ibid.* **14**, 1196 (1976).

[19] D.P. Landau and R.H. Swendsen, Phys. Rev. Lett. **46**, 1437 (1981).

[20] F.C. Alcaraz, J.R. Drugowich de Felício, R. Kóberle, and J.F. Stilck, Phys. Rev. B **32**, 7469 (1985).

[21] D.B. Balbão and J.R. Drugowich de Felício, J. Phys. A **20**, L207 (1987).

[22] J.C. Xavier, F.C. Alcaraz, D. P. Lara, and J.A. Plascak, Phys. Rev. B **57**, 11 575 (1998).

[23] P.D. Beale, Phys. Rev. B **33**, 1717 (1986).

[24] D. Friedan, Z. Qiu, and S. Shenker, Phys. Rev. Lett. **52**, 1575 (1984).

[25] J.L. Cardy, Nucl. Phys. B **270**, 186 (1986); **275**, 200 (1986).

[26] W. Press *et al.*, *Numerical Recipes* (Cambridge University Press, London, 1986).

[27] T. Tomé and M.J. de Oliveira, Phys. Rev. E **58**, 4242 (1998).

[28] K. Okano, L. Schülke, and B. Zheng, Found. Phys. **27**, 1739 (1997).

[29] Z.B. Li, L. Schülke, and B. Zheng, Phys. Rev. E **53**, 2940 (1996).

[30] D. Stauffer, Physica A **186**, 197 (1992).

[31] C. Münkel, D.W. Heermann, J. Adler, M. Gofman, and D. Stauffer, Physica A **193**, 540 (1993).

[32] L. Schülke and B. Zheng, Phys. Lett. A **215**, 81 (1996).

[33] R. da Silva, N. A. Alves, and J. R. Drugowich de Felício, Phys. Lett. **A298**, 325 (2002).

[34] O.F.D. Bonfim, J. Stat. Phys. **48**, 919 (1987).